AMERICAN JOURNAL OF PHYSIOLOGY
CELL PHYSIOLOGY

Am J Physiol Cell Physiol 322: C283–C295, 2022.
First published January 12, 2022; doi:10.1152/ajpcell.00350.2021

RESEARCH ARTICLE

Sex differences in the involvement of skeletal and cardiac muscles in myopathic *Ano5*$^{-/-}$ mice

Steven Foltz,[1] Fang Wu,[1] Nasab Ghazal,[2] Jennifer Q. Kwong,[1,2,3] H. Criss Hartzell,[1] and Hyojung J. Choo[1]

[1]*Department of Cell Biology, School of Medicine, Emory University, Atlanta, Georgia;* [2]*Department of Pediatrics, School of Medicine, Emory University, Atlanta, Georgia; and* [3]*Division of Pediatric Cardiology, Department of Pediatrics, School of Medicine, Emory University and Children's Healthcare of Atlanta, Atlanta, Georgia*

Abstract

Limb-girdle muscular dystrophy R12 (LGMD-R12) is caused by recessive mutations in the Anoctamin-5 gene (*ANO5, TMEM16E*). Although ANO5 myopathy is not X-chromosome linked, we performed a meta-analysis of the research literature and found that three-quarters of patients with LGMD-R12 are males. Females are less likely to present with moderate to severe skeletal muscle and/or cardiac pathology. Because these sex differences could be explained in several ways, we compared males and females in a mouse model of LGMD-R12. This model recapitulates the sex differences in human LGMD-R12. Only male *Ano5*$^{-/-}$ mice had elevated serum creatine kinase after exercise and exhibited defective membrane repair after laser injury. In contrast, by these measures, female *Ano5*$^{-/-}$ mice were indistinguishable from wild type. Despite these differences, both male and female *Ano5*$^{-/-}$ mice exhibited exercise intolerance. Although exercise intolerance of male mice can be explained by skeletal muscle dysfunction, echocardiography revealed that *Ano5*$^{-/-}$ female mice had features of cardiomyopathy that may be responsible for their exercise intolerance. These findings heighten concerns that mutations of ANO5 in humans may be linked to cardiac disease.

anoctamin-5; cardiomyopathies; LGMD-R12; skeletal myopathies; TMEM16E

INTRODUCTION

Recessive mutations in anoctamin-5 (*ANO5),* also known as transmembrane protein 16E (*TMEM16E*), cause limb-girdle muscular dystrophy R12 (LGMD-R12), Miyoshi muscular dystrophy-3 (MMD3), and mild muscle weakness and myalgia with elevated serum creatine kinase (CK) (1–3). These diseases are characterized by late-onset and mild to moderate muscle degeneration in the proximal or distal limbs with reduced muscle function. Despite not being genetically identified until 2010 (1, 2), *ANO5* myopathies are relatively common. For example, in a large American cohort of clinically suspected patients with LGMD, *ANO5* mutations were the 4th most likely contributor to LGMD phenotypes out of 35 LGMD genes (4). As the number of genetically identified LGMD-R12 cases has increased, the question has arisen whether cardiac pathology is also linked to *ANO5* mutations (5, 6). In a study of French patients with a genetically confirmed LGMD-R12 diagnosis, 31% had left ventricular dilation (7), whereas 32% of a group of Danish patients with *ANO5* mutations experienced moderate or high-frequency ventricular premature contractions (8). Recently, a genome-wide association study has identified *ANO5* as a genetic modifier of cardiomyopathy (9, 10).

ANO5 is a member of the anoctamin family that includes Ca^{2+}-activated Cl^- channels (11–13). However, ANO5 is not a Ca^{2+}-activated Cl^- channel, but rather, like its paralog ANO6 (TMEM16F), is a phospholipid scramblase that also carries ionic currents that are nonselective with regard to ionic species (14–16). Although the significance of ANO5-phospholipid scrambling (PLS) in muscle function is uncertain, previous studies indicated that ANO5 is important for muscle maintenance through processes that include muscle cell fusion and membrane repair (16–18). Recently, our group identified a domain within ANO5 required for both PLS and normal myoblast fusion (16), but this "scrambling domain" is not essential for proper muscle membrane repair by membrane patching (18). Other unidentified factors also contribute to *ANO5* myopathies (19). Although *ANO5* myopathy is not X-chromosome-linked, male prevalence of *ANO5* myopathy has been noted (20). Although differential effects of *ANO5* mutations in males and females have significant implications for therapy of *ANO5* myopathies, an analysis of sex-based differences has yet to be performed.

Here we show that female *Ano5*$^{-/-}$ mice are more resistant to exercise-induced muscle damage, and, unlike their male counterparts, have normal membrane patching after sarcolemmal wounding. However, female *Ano5*$^{-/-}$ mice exhibit exercise intolerance that can be explained by abnormal cardiac function. Taken together, *Ano5*$^{-/-}$ male and female mice exhibit differential susceptibility to skeletal and cardiac myopathies.

Correspondence: H. J. Choo (hchoo2@emory.edu); H. C. Hartzell (criss.hartzell@emory.edu).
Submitted 22 September 2021 / Revised 14 December 2021 / Accepted 7 January 2022

MATERIALS AND METHODS

Animals

Wild-type C57BL/6 male and female mice (9–12 mo old) were purchased from Jackson Laboratory. *Ano5* knockout mice were a gift from Dr. Louise Rodino-Klapac. *Ano5* knockout (KO) mice were backcrossed at least four times to C57BL/6 mice, before breeding to homozygosity (17). *Ano5* KO male and female mice (9–12 mo old) were genotyped using the following primers: for *Ano5* KO allele; F: 5′- AGTCCTTTTCAGCACAGTCTTTG-3′, R: 5′- TGAGGCA GTGTGGAGTGAGTA-3′. *Ano5* KO mice were maintained by breeding homozygotes. Both C57BL/6 and *Ano5* KO mouse colonies were fed with laboratory rodent diet 5001 and maintained with a 12:12 h dark:light cycle. Experiments involving animals were performed in accordance with approved guidelines and ethical approval from Emory University's Institutional Animal Care and Use Committee [PROTO20170233 (Choo), PROTO201800130 (Hartzell), and PROTO201700174 (Kwong)]. To harvest muscle tissues, mice were euthanized by an overdose of isoflurane. To minimize subjective bias, samples were blinded with arbitrary numbers.

Quantitative PCR

Approximately 10 mg of muscle tissues or nonmuscle tissues were isolated from mice and stored in −80°C freezer after snap freezing with liquid nitrogen. Total RNA was isolated with TRIzol (Invitrogen) according to the manufacturer's protocol. All RNA samples were treated with DNase I and the absence of DNA was confirmed by PCR. cDNA was synthesized by M-MLV reverse transcriptase (Invitrogen) using 1 μg of total RNA/sample and random hexamers as primers. cDNA was amplified using the SYBR select master mix (Applied Biosystems) and primers at a concentration of 2.5 μM. Amplified cDNA was detected and analyzed by StepOne software v2.2.2 (Applied Biosystems) using *Hprt* as an internal control. Fold change of gene expression was determined using the ΔΔCt method (21). Three to five independent experiments were performed. Sequence information of all primers for qPCR was designed using NCBI BLAST or PrimerBank. Primer sequences were:

Hprt F: 5′-TCAGTCAACGGGGGACATAAA-3′,
R: 5′-GGGGCTGTACTG CTTAACCAG-3′,
Ano5 (Ex22) F:'5- TCTTCCCACTGAGCACTTTC-3′,
R:'5-TGAGCATTCCTACACCAACC-3′,
Ano6 F:'5- CTTATCAGGAAGTATTACGGC-3′,
R:'5-AGATATCCATAGAGGAAGCAG-3′.

Primer sequences of each exon of ANO5 for reverse-transcription PCR were:

Ano5 Ex1/2–4 F:'5-AGCAGGAAGGCTTAACAGCCA-3′,
R:'5- AGACGCCTCCTCAGGAACAAA-3′,
Ano5 Ex5/6–7 F:'5- GCTGAAGGCAGAAAGAAGACG-3′,
R:'5- ACAGGGGTGGGTACTTTGGC-3′,
Ano5 Ex8/9–10 F:'5- TCCATGATGGCCAGTATTGGA-3′,
R:'5- CAGAGCCGCAAACAACAGCA-3′,
Ano5 Ex9-11/12 F:'5- GGAGCAACCTTTTCATTTGATTC-GG-3′,
R:'5- GGGAGAACTTTGAATGCAAAC-3′,
Ano5 Ex12-14/15 F:'5- TGCGCTCTTCATGGGGATCT-3′,
R:'5- GGAGAGCCATCCCAAAGGTCA-3′,
Ano5 Ex14/15–16 F:'5- ACAGTGACCTTTGGGATGGCT-3′,
R:'5- AGGCTGCTCTCATACTCCTGG-3′,
Ano5 Ex16/17–19 F:'5- AGCGAAGAGTGTGGTCCTGC-3′,
R:'5- CAAACAGGGGTGCCAGAGGA-3′,
Ano5 Ex19/20–21 F:'5- ATCGTTTCTGTTGCAACTAATGC-CT-3′,
R:'5- TGGCAGCAAGAACATGCCAG-3′,
Ano5 Ex22 F:'5- CCTGGCTGATACCAGATGTTCCTA-3′,
R:'5- GCATCCAGCCTGAAACCCAGA-3′.

Tissue Histology and Immunostaining

Muscle tissues were frozen in Tissue Freezing Medium (Triangle Biomedical Sciences) and stored at −80°C. Tissue cross sections of 10 μm thickness were collected every 200 μm for gastrocnemius (GA) muscles using a Leica CM1850 cryostat. To quantify myofiber cross-sectional areas of specific fiber types from GA muscles, tissue sections were fixed in freshly prepared 4% paraformaldehyde (Electron Microscopy Sciences). Subsequently, the M.O.M. Kit (Vector Laboratories Inc.) was used to block endogenous Fc receptor binding sites followed by a 1 h incubation with 10% goat serum, 1% BSA, and 0.25% Triton-X100 in PBS (blocking buffer). Sections were then labeled with a solution containing a 1:1:1 mixture of anti-MHC I [No. BA-D5, supernatant, Developmental Studies Hybridoma Bank (DSHB), RRID: AB-2235587 (22)]: anti-MHC IIa [No. SC-71, supernatant, DSHB, RRID: AB-2147165 (22)]: anti-MHC IIb [No. BF-F3, supernatant, DSHB, RRID: AB-2266724 (23)] plus anti-laminin (No. 9393, final concentration 2 μg/mL, Sigma, RRID: AB-477163) overnight at 4°C. After washing with PBS containing 0.2% Tween-20, secondary antibodies were applied for 60 min at room temperature. Secondary antibodies were used at a 1:200 dilution (Invitrogen). Secondary antibodies were: Alexa Fluor (AF) 350-conjugated goat-anti-mouse $F(ab')_2$ IgG_{2b} fragments (No. A21140, final concentration 10 μg/mL), AF647-conjugated goat-anti-mouse $F(ab')_2$ IgG_1 fragments (No. A21240, 10 μg/mL), AF488-conjugated goat-anti-mouse $F(ab')_2$ IgM fragments (No. A21042, 10 μg/mL) and AF594-conjugated donkey anti-rabbit $F(ab')_2$ IgG fragments (No. A21207, 1.5 μg/mL). Nuclei were then stained with 4',6-diamidino-2-phenylindole (DAPI, 1 μg/mL for 3 min). Sections were mounted with Vectashield (Vector Labs). To minimize bias for histological analysis, we blinded samples with arbitrary numbers and used an automated muscle histology analysis software, Myosoft (24), to analyze all the muscle fibers in gastrocnemius muscle sections (7,000–8,000 fibers/tissue).

Treadmill and CK Assay

Mice were acclimatized to the treadmill environment (Columbus Instruments) on consecutive days. The first session involved placing the mice within treadmill lanes for 30 min without belt movement and with electrical shock pads off, whereas the second session involved 30 min of belt movement at 2 m/min with electrical shock pads on. One day after acclimatization, mice were exercised at 10 m/min for 1 h at 10° decline. Incidents of stopping on shock pads for greater than 1 s were recorded up to a maximum of 75 stops,

after which mice were removed from the treadmill and a stop time was recorded. A week before exercise and 30–60 min post exercise, 20–40 μL of blood was collected through tail vein bleeding after numbing the tail locally with ice-cold ethanol. This time for blood collection was chosen because maximal CK levels were found to occur 30–60 min after exercise in mdx mice (25). Serum was isolated by centrifugation (10,000 *g* for 5 min at 4°C) for analysis by CK assay. CK activity was determined according to the manufacturer's protocol (Stanbio Laboratory). Briefly, absorbance at 340 nm was detected at every 30 s for 2 min at 37°C. The changed absorbance per minute was used to calculate enzyme activity.

Membrane Damage Assay

As described previously (18), flexor digitorum brevis muscles from wild-type and sex-matched *Ano5*$^{-/-}$ mice were dissected on the same day and digested at 37°C in 0.2% Collagenase A (Roche) in DMEM supplemented with 25 mM HEPES for 3 h. Digestion was terminated by addition of 10% BSA, and single muscle fibers were released by mechanical agitation. Fibers were seeded onto Matrigel (Corning) coated glass-bottomed culture dishes (MatTek) for at least 30 min before imaging. Imaging buffer consisted of 1.8 mM $CaCl_2$, 0.8 mM $MgSO_4$, 5.3 mM KCl, 44 mM $NaHCO_3$, 110 mM NaCl, 0.9 mM NaH_2PO_4, 1 mM sodium pyruvate, 5.6 mM D-glucose, and MEM amino acids solution (Thermo Fisher, used at 2X final concentration) supplemented with 0.4 mM L-serine, 0.4 mM glycine, 4 mM L-glutamine, and 2.5 μM FM1-43 (Thermo Fisher), a lipophilic dye monitoring membrane repair. Imaging dishes containing isolated muscle fibers were placed in a stage-top incubator (Tokai-Hit) heated to 37°C and gassed with 95% air/5% CO_2. All images were taken on a Nikon A1RHD25 scanning confocal microscope using a ×60 1.4 NA oil objective. A 2 μm × 2 μm (24.1pixel × 24.1pixel) region of interest was specified at the lateral edge of the fiber for laser ablation. Fibers were irradiated with a 405 nm laser set to 100% power (corresponding to ~0.9 - 1.1 mW) for 8 s. Images were acquired in Nikon Elements software once immediately before and after injury, then for every 4 s for a total of 2 min (32 images total), and finally every 15 s for a total of 5 min (21 images total). Times are reported as time from the start of scanning image No.1 (preinjury) $t = 0$.

Echocardiogram

Echocardiography was conducted as described previously (26). Briefly, mice were anesthetized by isoflurane inhalation with body temperature maintained at 37°C. Measurements were performed using a Vevo 2100 Imaging System (Visual Sonics) equipped with a MS-400 transducer. M-mode measurements were taken of the parasternal short-axis view. Systolic and diastolic ventricular chamber dimensions, ventricular wall, and septal thicknesses were assessed, and fractional shortening was calculated using VevoLab software.

Statistics

Statistical significance was determined via unpaired Welch's *t* test for two groups or one-way ANOVA with Tukey's posttest correction for three or more groups. The significance of the results obtained from multiple groups with an additional factor was evaluated by two-way ANOVA with Sidak's multiple-comparisons test. Statistical analyses were performed using Prism 8 software (GraphPad). A *P*-value of less than 0.05 was considered significant.

RESULTS

Male Patients with ANO5 Myopathies Exhibit Increased Skeletal and Cardiac Muscle Pathology

We analyzed 22 published articles published between 2010 and 2021 reporting skeletal and/or cardiac muscle pathologies of patients with LGMD-R12. Since we focus on sex differences in myopathy of patients with LGMD-R12, we excluded a report without sex information of recruited patients. If studies presented age range instead of exact age, we used the median value of the range. The meta-analysis from 2010 to 2021 revealed that 74.3% of 404 genetically diagnosed patients with ANO5 myopathy are male (Fig. 1*A*, Supplemental File S1; see https://doi.org/10.6084/m9.figshare.16661206.v3) (1, 3, 5, 7, 8, 19, 20, 27–40). Age of onset of male patients (33.7 ± 0.7) averaged 3 yr younger than in females (36.7 ± 1.6) (Fig. 1*B*). Females are more likely to present as "asymptomatic" with hyperCKemia with no skeletal muscle symptoms beyond mild myalgia (33%) compared with males (17%). Most asymptomatic male patients were younger than 40 yr, whereas over half of asymptomatic female patients were older than 40 yr (Fig. 1, *C* and *D*). This suggests that myopathy develops more slowly in females than in males. Male patients with *ANO5* mutations were more likely to show cardiac symptoms (16%) than female patients (9%), but females with cardiac abnormalities are 8.5 yr younger than male patients on average, although the group of female patients with cardiac involvement is small (Fig. 1, *E* and *F*). On average, male patients with cardiac symptoms were older than patients with no cardiac symptoms. In contrast, female patients with cardiac abnormalities tended to be younger than both male symptomatic patients and female asymptomatic patients. Our analysis confirms male prevalence of both skeletal and cardiac pathologies in patients with *ANO5* mutations and suggests that age correlates with skeletal and cardiac myopathy in male patients.

Skeletal Muscle Pathology Is Reduced in *Ano5*$^{-/-}$ Female Mice

This meta-analysis of the research literature suggests that sex modifies the manifestation of symptoms caused by disruption of the *ANO5* gene, but these sex differences can be explained in many diverse ways. To explore the involvement of sex in *ANO5* myopathy further, we compared males and females in a mouse model of *ANO5* myopathy (17). Because elevated serum creatine kinase is a diagnostic feature of LGMD-R12, we first measured serum creatine kinase before and after mice had exercised on a treadmill (Fig. 2*A*). Although creatine kinase was significantly increased in *Ano5*$^{-/-}$ male mice after exercise (2-fold), there was no difference between wild-type and *Ano5*$^{-/-}$ females.

Increased serum creatine kinase occurs when muscle fibers become damaged and release cytoplasmic contents. We have previously shown that membrane repair in male *Ano5*$^{-/-}$ mice is impaired (18) and proposed that the increased serum creatine kinase is caused by this defective

membrane repair. To determine whether male and female mice differ in their ability to repair damaged sarcolemma, we assayed the ability of isolated myofibers to repair damage caused by an intense 405 nm laser pulse as described previously (18). We used a common damage assay based on the cell-impermeant dye FM1-43 (41–47). FM1-43 is a water-soluble stearyl dye that is not fluorescent in aqueous solution, but fluoresces intensely when inserted into lipid-rich membranes. When the sarcolemma is damaged, FM1-43 enters the cell, labels internal membranes, and produces a bright fluorescent spot around the site of injury. If the membrane is repaired, the quantity of dye entering the fiber is attenuated compared with fibers where repair is defective (Fig. 2*B*). As we have previously reported, FM1-43 fluorescence increases after injury two to three times more rapidly in *Ano5*$^{-/-}$ male muscle fibers than in wild type (18). However, FM1-43 fluorescence increases at the same rate in WT and *Ano5*$^{-/-}$ females (Fig. 2, *C* and *D*). This rate is very similar to that observed in WT males. This suggests that membrane repair in male Ano5 KO mice is more severely affected than in female Ano5 KO mice.

Male and Female *Ano5*$^{-/-}$ Mice Exhibit Similar Exercise Intolerance

To determine whether ANO5-deficient muscles were functionally different between males and females, we challenged mice with a downhill treadmill run for up to 60 min. Both male and female *Ano5*$^{-/-}$ mice stopped running more frequently than sex-matched WT animals and they ran for shorter periods of time before they exceeded the threshold of 75 stops (Fig. 3). It is also notable that the performance of KO animals was considerably more variable than WT animals. This recapitulates the variability in clinical symptoms in the human LGMD-R12 population. Although WT males and females performed similarly on the treadmill, *Ano5*$^{-/-}$ females stopped more frequently and ran for significantly less time than WT females or males (Fig. 3, Supplemental File S2). These results are consistent with the conclusion that *Ano5*$^{-/-}$ males have a skeletal muscle dysfunction that prevents them from running consistently on a treadmill. However, because *Ano5*$^{-/-}$ female mice do not exhibit elevated serum creatine kinase or defective membrane repair, it seemed unlikely that their reduced performance was related to skeletal muscle defect. Therefore, we performed additional experiments to understand the reduced exercise performance of *Ano5*$^{-/-}$ females.

Ano5$^{-/-}$ Mice Do Not Exhibit Muscle Atrophy

To examine the anatomical features of Ano5-myopathy in mice, we undertook a histological examination of muscle fibers from male and female *Ano5*$^{-/-}$ mice. To minimize bias for histological analysis, we used an automated muscle histology analysis software, Myosoft (24), to analyze all the

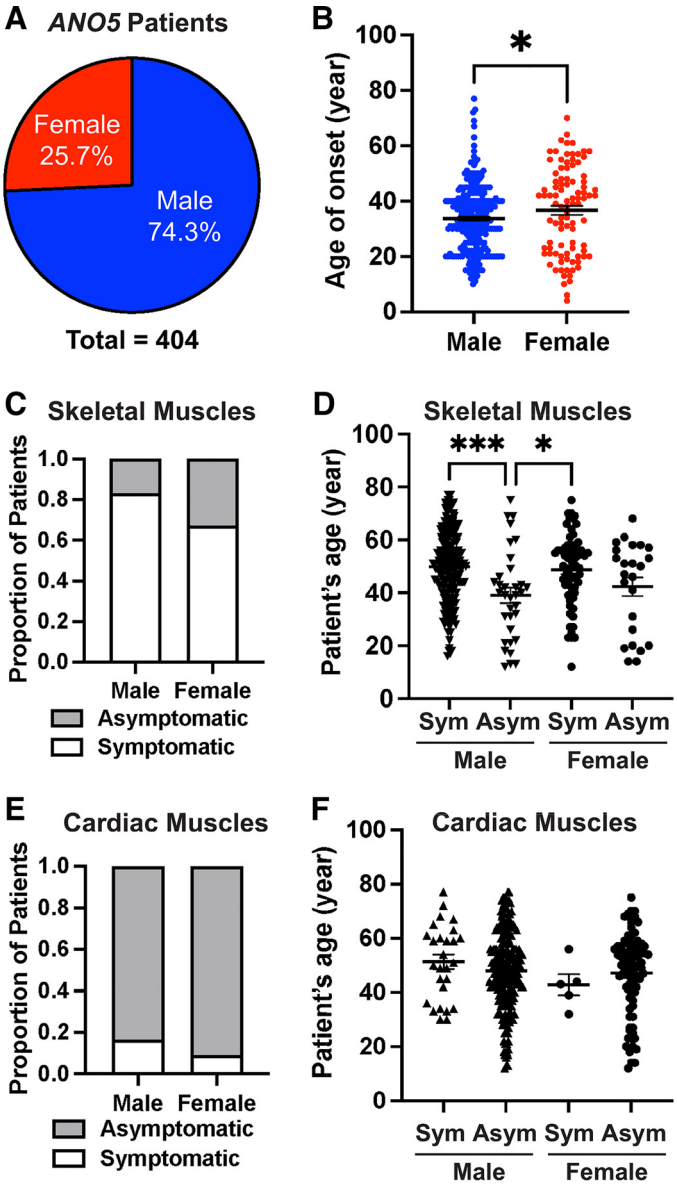

Figure 1. Clinical data analysis of patients with ANO5 myopathy. Published data from 21 clinical case reports published between 2010 and 2021 were analyzed. *A*: percentage of male and female patients with LGMD-R12. Of a total 404 genetically diagnosed patients with ANO5 myopathy, male patients represented 74.3% and female patients represented 25.7%. *B*: average age of onset of male patients is 3 yr earlier than female patients Welch's *t* test was used for statistical analysis. *C*: morphological and functional analyses of skeletal muscles from 404 patients with sex information were performed in 22 clinical case studies. Asymptomatic was defined as no pathological symptoms with or without elevated serum creatine kinase levels. Approximately 83% of male patients and 67% of female patients exhibited skeletal muscle pathologies, which were measured by electromyography, MRI/CT, or muscle biopsy. *D*: age of male and female patients with symptom or without symptom of skeletal pathology. *E*: morphological and functional analysis of cardiac muscles were performed on 268 patients with sex information in 15 clinical case studies. Asymptomatic was defined as no morphological and functional abnormalities from electrocardiography and echocardiography. Approximately 16% of male patients and 9% of female patients exhibited cardiac muscle pathologies such as left ventricle hypertrophy. *F*: age of male and female patients with symptom or without symptom of cardiac abnormality. Data are represented as means ± SE. One-way ANOVA with Tukey's multiple-comparisons test was used to determine statistical significance. $*P < 0.05$, $***P < 0.001$. ANO5, Anoctamin-5; CT, computerized tomography; LGMD-R12, limb-girdle muscular dystrophy R12.

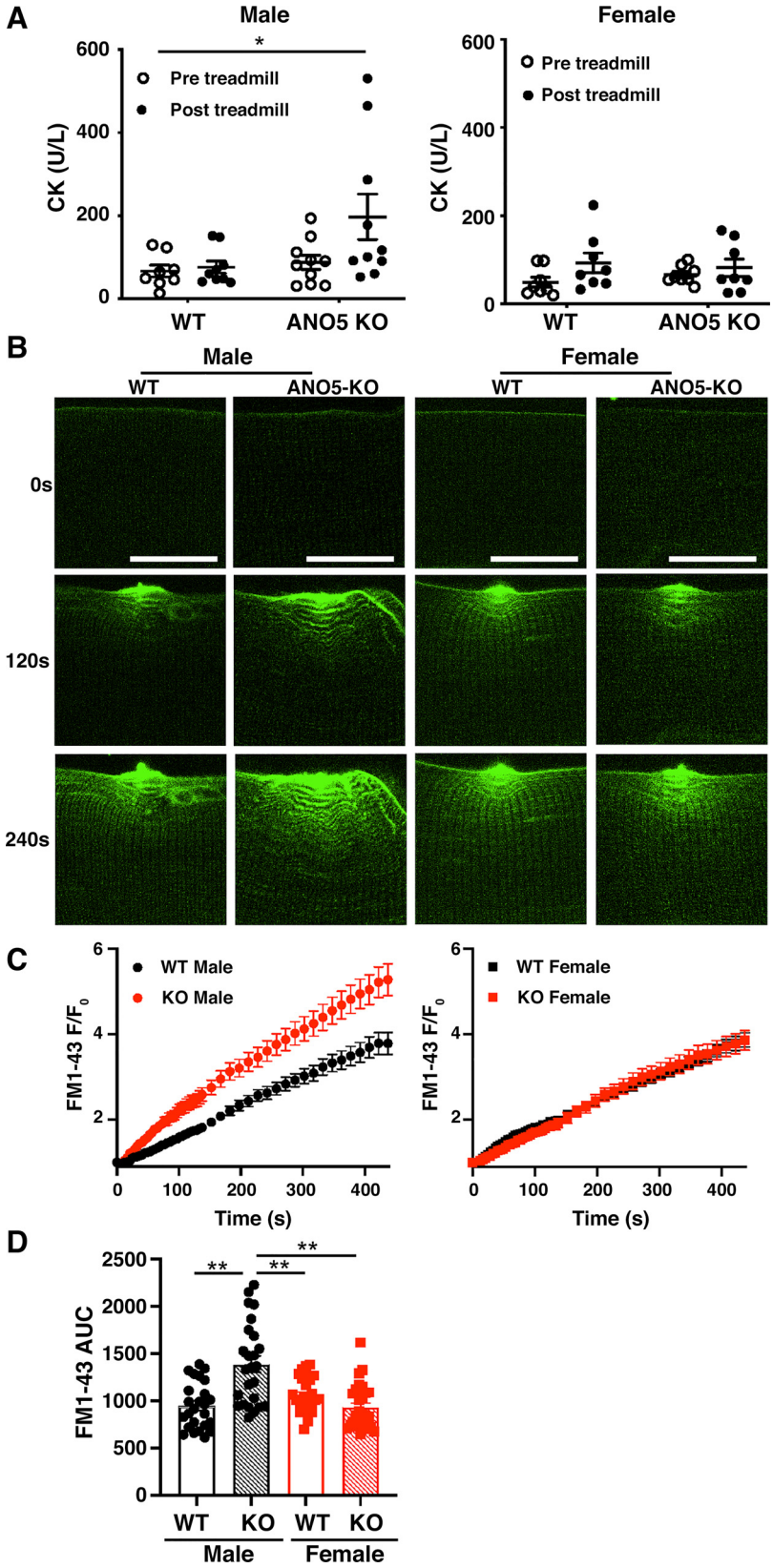

Figure 2. Skeletal muscle pathology is reduced in female *Ano5*$^{-/-}$ mice. *A*: *Ano5*$^{-/-}$ male showed higher serum CK levels after exercise; n = 8–10 animals per group. Two-way ANOVA with Tukey's multiple-comparisons test was used to determine statistical significance. *B*: representative images of FM1-43 infiltration at indicated time following membrane damage in WT or *Ano5*$^{-/-}$male and female fibers. Scale bar = 10 μm. *C*: time course of FM1-43 fluorescence normalized to initial fluorescence before laser-induced damage in WT and *Ano5*$^{-/-}$ male (*left*) and female (*right*) fibers. *D*: area under the curve (AUC) in *E* for individual WT or *Ano5*$^{-/-}$ fibers. WT: n = 27–30 fibers pooled from three mice of each sex. *Ano5*$^{-/-}$: n = 25 fibers pooled from three mice of each sex. Data are represented as means ± SE. One-way ANOVA with Tukey's multiple-comparisons test was used to determine statistical significance. *$P < 0.05$ and **$P < 0.01$. CK, creatine kinase; WT, wild type.

muscle fibers in gastrocnemius muscle sections (7,000–8,000 fibers/tissue). Muscle fiber cross-sectional area (CSA) was not different between WT and *Ano5*$^{-/-}$ sex-matched mice, although males of both genotypes had significantly larger CSAs than females of the respective genotype (Fig. 4). Because muscles are composed of several different metabolic types of muscle fibers and differences within one fiber type might not be revealed in averages of the fibers in an entire

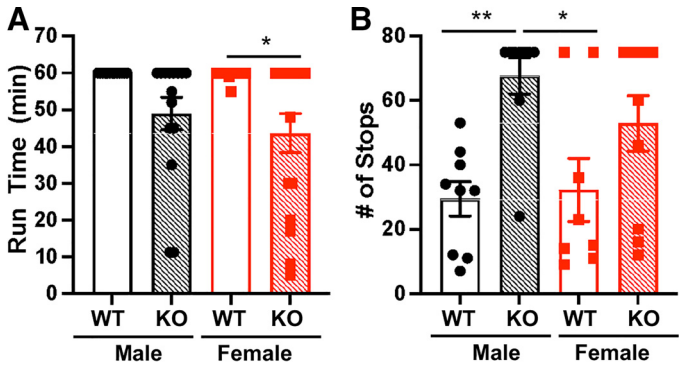

Figure 3. Exercise intolerance of male and female *Ano5*$^{-/-}$mice. *A*: WT and *Ano5*$^{-/-}$ male and female mice were exercised on a treadmill running at 10 m/min for 1 h with 10° decline. Running time was measured for 60 min or until animals stalled on shock pads (>1 s) 75 times. *Ano5*$^{-/-}$female mice showed significantly shorter running time compared with WT female mice; n = 11–16. *B*: an exercise stop was counted when a mouse stopped running and occupied the shock pad for >1 s. After 75 stops, mice were removed from the treadmill and the trial ended. *Ano5*$^{-/-}$ male mice showed significantly higher stopping numbers than WT mice of both sexes but were not significantly different from *Ano5*$^{-/-}$ females; n = 8–10 animals. Data are represented as means ± SE. One-way ANOVA with Tukey's multiple-comparisons test was used to determine statistical significance. WT, wild type.

muscle, we evaluated myofiber CSAs by fiber type. Fiber types (I, IIa, IIb, and IIx) were defined by staining with antibodies against fiber-type specific myosin heavy chain. No differences between WT and *Ano5*$^{-/-}$ were found (Fig. 4 and Supplemental File S3), indicating that muscle atrophy is not present in 9–12-mo-old *Ano5*$^{-/-}$ mice of either sex. This result was unexpected because we previously reported that the diameters of both gastrocnemius and tibialis anterior *Ano5*$^{-/-}$ mice was less than WT (17), but in these previous studies, animals were not sex-matched, so differences may be explained by unequal male-female ratios in different genotypes.

Ano5$^{-/-}$ Male and Female Mice Have Divergent Cardiac Phenotypes

One explanation to reconcile the reduced exercise performance of *Ano5*$^{-/-}$ females with their apparent normal skeletal muscle function and histopathology is that ANO5 deficiency manifests in other tissues in females. Because it has been suggested that patients with LGMD-R12 exhibit a higher-than-expected incidence of cardiovascular disorders (7, 8), we examined cardiac function of 10-mo-old live mice by echocardiography. All of the echocardiogram-derived parameters for male mice were the same for WT and *Ano5*$^{-/-}$ (Fig. 5, *B*, *D*, and *F* and Supplemental File S4). In contrast, female *Ano5*$^{-/-}$ mice had significantly smaller left ventricular end-diastolic volume (LVEDV), smaller left ventricular internal diameter (LVID), and larger left ventricular end volume anterior wall thickness (LVAW) (Fig. 5, *C*, *E*, and *G*). The reduction in LVID and increased LVAW along with a trend for increased LV posterior wall diameter (data not shown) is indicative of cardiac hypertrophy and is consistent with *Ano5*$^{-/-}$ female mice having a decrease in cardiac function that may lead to exercise intolerance. However, we did not observe fibrosis or other abnormalities in cross-sectioned hearts stained with Masson's trichrome or hematoxylin and eosin in any group.

ANO5 Expression Is Similar in Male and Female and Decrease with Age in Limb Muscles

To determine whether differences in ANO5 expression in males and females might explain the differences in phenotype, we quantified the expression of *Ano5* in several different muscles and tissues from mice of different ages using quantitative real-time PCR (qRT-PCR). *Ano5* transcript levels were not different between male and female mice of the same age (3 mo or 22 mo) in quadriceps, but in gastrocnemius muscles, *Ano5* expression was statistically higher in females than males. Skeletal muscles are derived from two different developmental origins (somite and pharyngeal arches) and have distinct transcriptional profiles reflective of their specialized roles within the body (48), so we tested both limb and craniofacial muscles. Overall, *Ano5* transcripts in young male quadriceps and gastrocnemius muscles were significantly higher than transcripts in craniofacial muscles such as tongue and pharynx of young or old mice of either sex (Fig. 6*A*, note different scales). Consistent with previous reports (49), *Ano5* expression was greater in limb muscles than in other tissues, including brain, kidney, and liver (Supplemental File S5). ANO5 expression was significantly lower in limb muscles from older mice but not in craniofacial muscles and other tissues.

To evaluate *Ano5* expression in heart, we used RT-PCR to confirm that all exons of *Ano5* are expressed in heart (Fig. 6*B*). We found that female hearts contained less *Ano5* mRNA than male hearts (Fig. 6*C*). Differences in ANO5 expression do not obviously explain differences in phenotype between male and female mice.

DISCUSSION

The muscular dystrophies are highly heterogenous at the clinical level, but factors underlying this phenomenon are poorly understood. In particular, the contributions of biological sex to pathology of autosomal muscle disease are infrequently investigated despite clear physiological differences in skeletal muscles of males and females. Furthermore, disease comorbidities may differ between males and females, affecting patient care and outcomes. Although we previously demonstrated recapitulation of LGMD-R12 phenotypes in *Ano5*$^{-/-}$ mice (17), we did not consider sex as a biological variable. Some of our previous findings, such as reduced myofiber sizes in *Ano5*$^{-/-}$ mice, were reversed upon sex-based stratification by unbiased analysis; myofiber size was sex-dependent but not genotype-dependent (Fig. 4). In the present study, we determined that while *Ano5*$^{-/-}$ female mice were resistant to muscle damage following a downhill treadmill run, which is a physiologically relevant assay for use-induced muscle damage in vivo (Fig. 2). One possibility is that smaller myofibers of female mice generate less force per contraction and consequently deliver less lateral strain to the muscle plasma membrane. However, our finding that male, but not female *Ano5*$^{-/-}$ muscle fibers had increased susceptibility to laser-induced damage in vitro (Fig. 2)

suggests a bona fide difference between male and female *Ano5*$^{-/-}$ muscles. Despite lacking this key phenotype, female *Ano5*$^{-/-}$ mice exhibited exercise intolerance (Fig. 3). We hypothesized that abnormalities in cardiac rather than skeletal muscle explain poor treadmill performance. In support of this idea, our mouse studies showed differential cardiac function between male and female KO mice (Fig. 5).

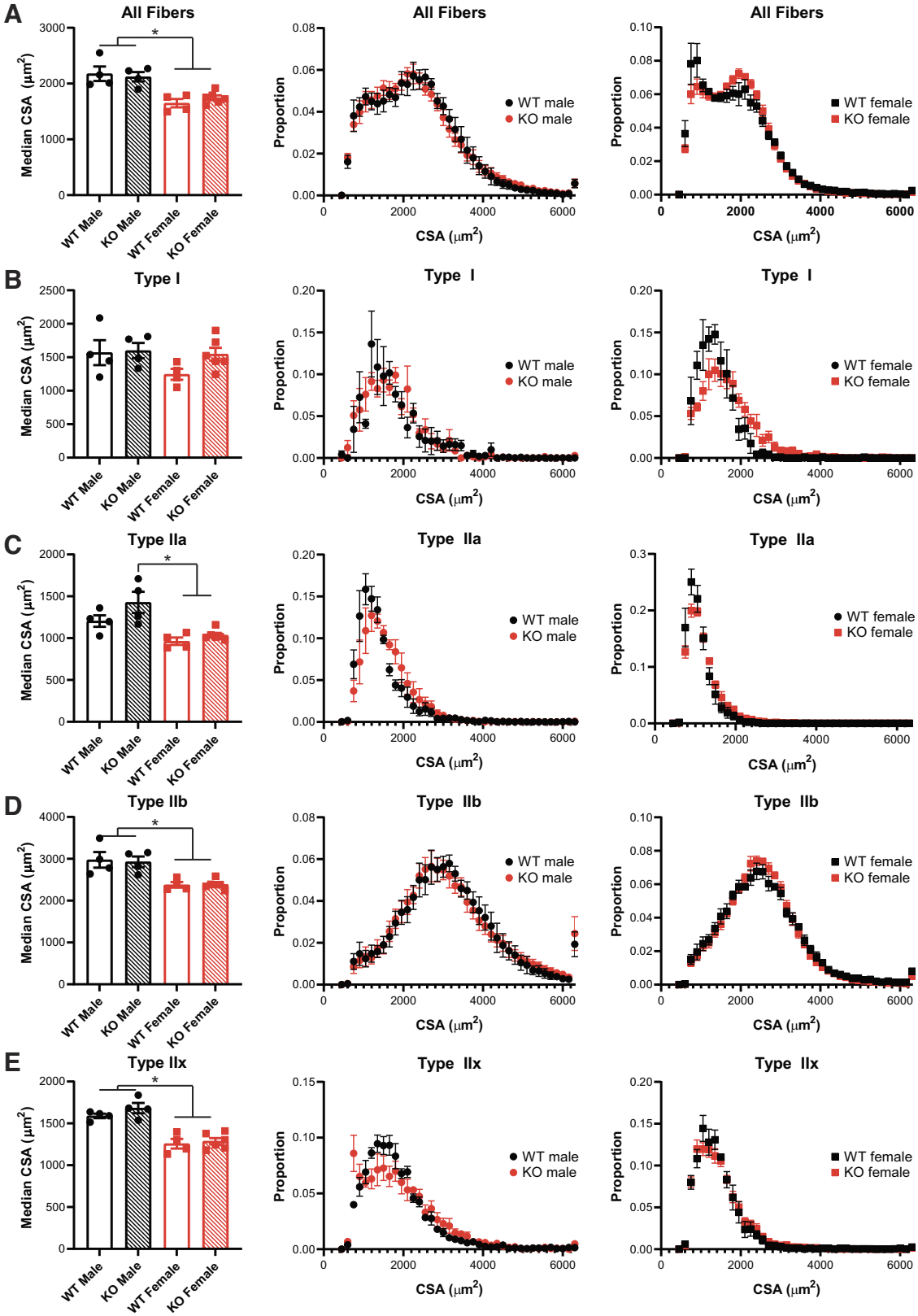

Our meta-analysis of the literature showed that both skeletal and cardiac pathologies were more commonly reported in male than female patients with LGMD-R12 (Fig. 1). This is the opposite of what we would expect based on our mouse data. One likely explanation is that the number of female patients is underestimated due to mild or asymptomatic skeletal muscle pathologies, which make females less likely to receive a genetic diagnosis. *ANO5* is located on an autosomal chromosome (11p14.3), and males and females should thus be equally likely to harbor a mutant allele. The finding that fewer females present in the clinic supports that disease symptoms are less penetrant in females. Furthermore, several published pedigrees show that females with *ANO5* mutations are less likely to have myopathic symptoms (3, 37). However, other possible reasons for this sex difference might be considered. One possibility is that males may be more likely to perform activities that might induce more severe muscle damage. Anecdotally, some patients with *ANO5* mutations report high-level athletic activity in their lives before presenting with LGMD-R12 (50).

It should be stressed that while the exercise intolerance of female *Ano5*$^{-/-}$ mice may be explained by the presence of cardiomyopathy, there is currently no evidence that such a correlation exists in humans. It is possible that not all findings in the mouse model will extend to humans, but this can only be determined on an empirical basis. Nevertheless, studies using other mouse models of muscular dystrophy have demonstrated congruency between animal and human cardiac phenotypes. A prominent example of this is the case of dysferlinopathy (51), a class of muscle disease with clinical, histological, and mechanistic similarities to ANO5 myopathies. Unlike ANO5 myopathies, male and female patients are equally affected in dysferlinopathy (52), and divergent phenotypes have not been noted in male and female dysferlin-deficient mice, which are used interchangeably (51, 53–55). Dysferlin deficiency is linked to cardiomyopathy in both male and female patients, though cardiac involvement is not a universal feature of dysferlinopathy (52, 56–58). Similarly, although dysferlin participates in cardiomyocyte membrane repair, echocardiography revealed that dysferlin-KO mice have only late-onset, mild cardiomyopathy (53, 54). In *mdx* mice, a common model of Duchenne muscular dystrophy, echocardiography has demonstrated that cardiac pathology is relatively late onset (59, 60), which is consistent with the human disease where skeletal muscle involvement precedes cardiomyopathy by several years (61). In many cases, histopathological changes will occur before measurable functional changes. In β-sarcoglycan-KO mice, a model for LGMD-R4, echocardiography of adult mice returned normal results, while aspects of cardiomyopathy were noted following histological analysis (62, 63). Fatal cardiomyopathy has been reported in young adult patients with β-sarcoglycan mutations (64), highlighting another important caveat to interpreting mouse studies: even when phenotypes match between humans and animal models, disease timing cannot be easily extrapolated from animals to humans.

Currently, 72 *ANO5* mutations have been identified as pathogenic; however, it remains unclear how these mutations cause pathology partly because the correlation between genotype and phenotype in patients is erratic and the phenotypes of *ANO5* myopathy animal models are controversial. Furthermore, a significant fraction of patients with LGMD-R12 also has mutations in other neuromuscular disease-associated genes (4). Two animal models using complete knockout methods show no muscle pathology but a mouse model generated by gene trapping between exon 8 and exon 9 (17) and a CRISPR/Cas9 rabbit KO model with open reading frame disruption of exons 12 and 13 (65) recapitulate the human pathology. Dominant *ANO5* mutations cause a bone disease known as ganthodiaphyseal dysplasia (GDD), rather than myopathy (49, 66, 67). Until recently, it was believed that muscle- and bone-disease-causing mutations were distinguished by loss versus gain of function at the protein level, specifically with respect to the PLS activity of ANO5 (68, 69). However, this model is complicated by the presence of the PLSase ANO6 in muscle, which apparently fails to compensate for the loss of ANO5. Furthermore, we recently reported that muscle membrane repair proceeds independently of ANO5-PLS (18). Thus, even with recent progress in understanding ANO5-related disease mechanisms, outstanding questions remain.

Myriad factors contribute to the complex manifestations of genetic diseases in humans. Genetic modifiers represent a prominent example of this: variants of "unaffected" genes can dramatically influence disease courses in patients (70). Recently, mutations in *ANO5* have been recognized as a genetic modifier of cardiomyopathy in patients with hereditary neuromuscular diseases using next-generation sequencing analysis (9, 10). From a Scottish genome-wide association study, single-nucleotide polymorphisms of *ANO5* were associated with elevation of cardiac troponin I, which is a strong risk factor for cardiovascular disease (10). Both reports emphasize the role of ANO5 for cardiac muscle functions. Our literature review concludes that ~15% of patients with *ANO5* mutations exhibit some cardiomyopathy, which is much higher than the prevalence of cardiomyopathy in the general population (~0.2%). Altogether, available evidence suggests that *ANO5* mutations are linked to cardiomyopathy. In the future, defining the mechanisms by which other disease modifiers, such as aging and biological sex, alter pathophysiology will likewise carry potential for developing treatments.

Conclusions

Ano5$^{-/-}$ model mice exhibit male-dominant skeletal muscle phenotypes of ANO5 myopathies. Female *Ano5*$^{-/-}$ mice have reduced skeletal muscle pathology compared with

Figure 4. No evidence of muscle atrophy in *Ano5*$^{-/-}$mice. Gastrocnemius muscles were isolated from 9–12-mo-old WT and *Ano5*$^{-/-}$male and female mice. Gastrocnemius muscles were sectioned and immunostained with anti-laminin, and antibodies to type I, IIa, and IIb myosin heavy chain. Cross-sectional areas (CSA) of whole muscle sections (*A*) and specific fiber types (*B–E*) were analyzed by Myosoft, an automatic muscle histology analysis program (24); n = 4–6 animals for each group. Approximately 7,000–8,000 myofibers were analyzed for each muscle section. Data are presented as means ± SE. Two-way ANOVA with Sidak's multiple-comparisons test was used to determine statistical significance. *$P < 0.05$ compared with male and female group. WT, wild type.

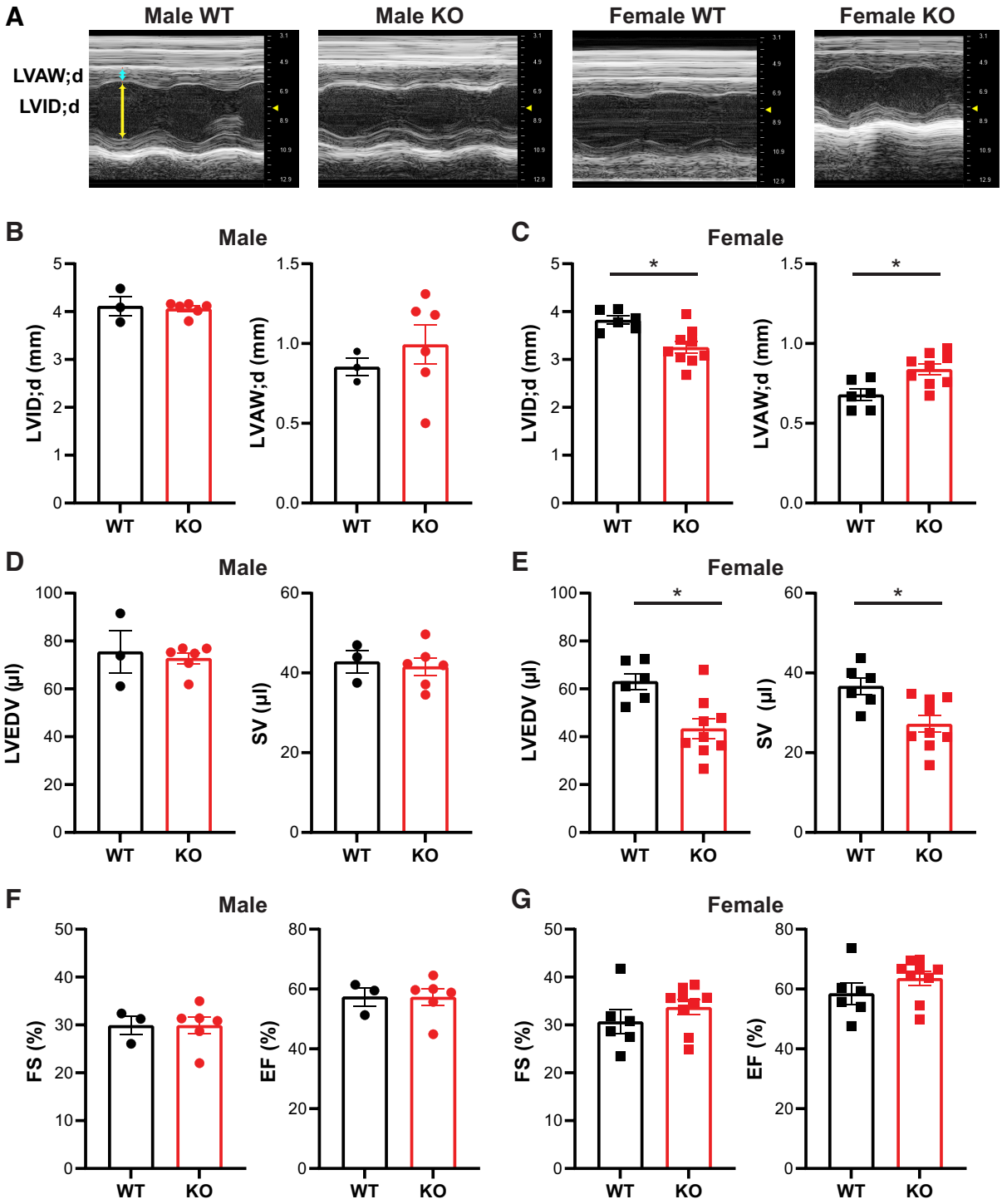

Figure 5. *Ano5*$^{-/-}$KO female mice have left ventricle hypertrophy. *A*: representative image of echocardiogram (M mode) of WT and *Ano5*$^{-/-}$male and female heart. *B*: echocardiograms were performed on 10-mo-old mice to measure left ventricle (LV), interior diameter (LVID), and left ventricle anterior wall diameter (LVAW) (*B* and *C*); LV end-diastolic volumes (LVEDV) and stroke volumes (SV) (*D* and *E*); and ejection fraction (EF) and fractional shortening (FS) (*F* and *G*). *Ano5*$^{-/-}$female mice exhibited left ventricle hypertrophy compared with WT female. n= 3–6 animals for male groups and n = 6–9 animals for female groups. Data are presented as means ± SE. Welch's t test was performed to determine statistical significance. *$P < 0.01$. KO, knockout; WT, wild type.

male mice. Female KO mice are more resistant to exercise-induced muscle damage and normal membrane patching after sarcolemmal wounding but show exercise intolerance. Female *Ano5*$^{-/-}$ mice exhibit abnormal cardiac morphology, such as left ventricular hypertrophy, which may account for reduced performance in a treadmill functional assay. Therefore, male and female mice can be used to study relevant (skeletal or cardiac) pathology of *ANO5* myopathies. The mechanism of sex-differential effects of *ANO5* mutations may hold clues for therapeutic development in the future.

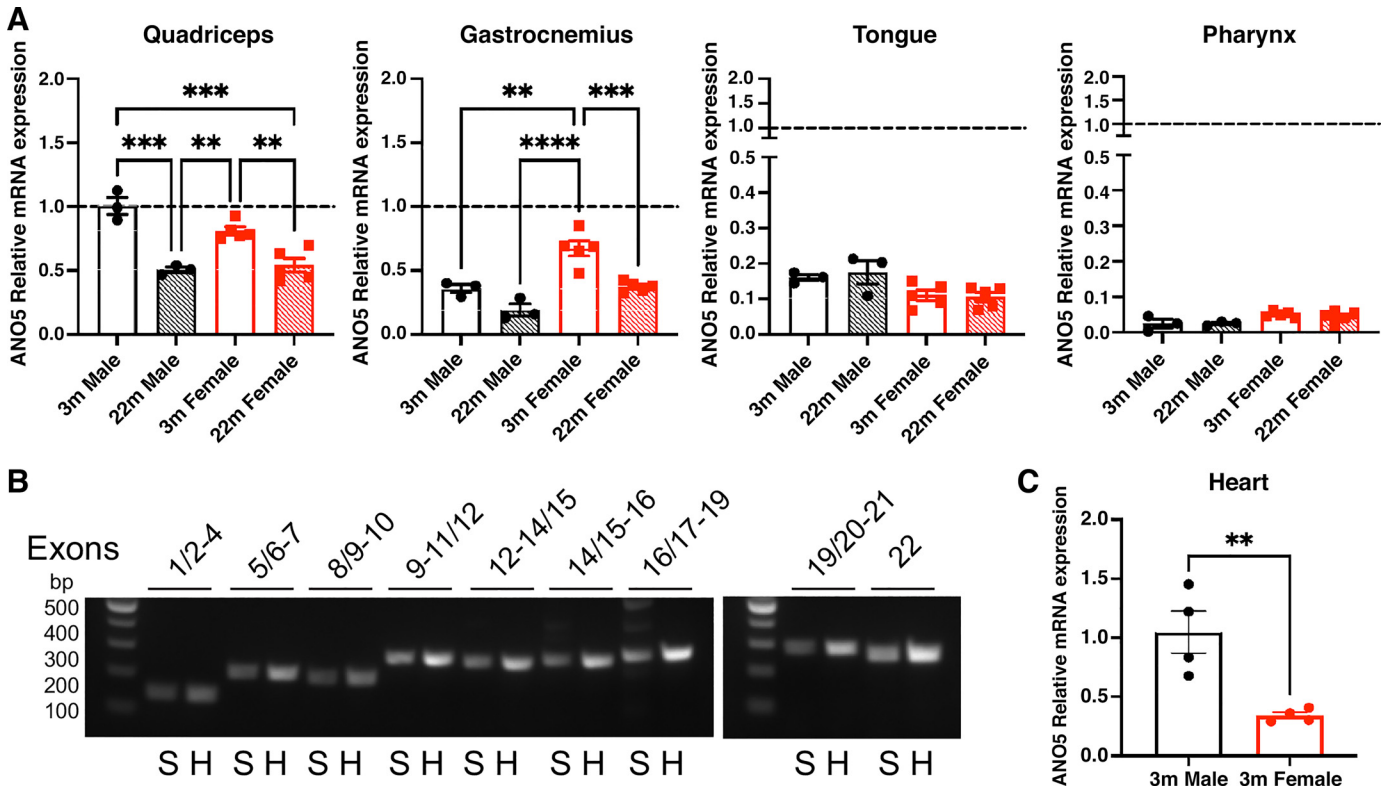

Figure 6. ANO5 is highly expressed in limb muscles and decreases with age. *A*: steady state level of *Ano5* mRNA was measured from quadriceps, gastrocnemius, tongue, and pharyngeal muscles of 3- and 22-mo-old male and female C57BL/6 mice. Relative expression was normalized to a housekeeping gene, *Hprt*, and resulting values were compared with the level of *Ano5* mRNA levels in quadriceps of 3-mo-old males, which is indicated by a dashed line; $n = 3–5$ animals. Data are represented as means ± SE. One-way ANOVA with Tukey's multiple-comparisons test was used to determine statistical significance. $^{**}P < 0.01$, $^{***}P < 0.001$, $^{****}P < 0.0001$, $\#P < 0.05$ compared with 3-mo-old quadriceps, $\$P < 0.05$ compared with 3-mo-old gastrocnemius. *B*: expression of all ano5 exons in 3-mo-old heart were confirmed by RT-PCR. S indicates skeletal muscle tissues as control tissues and H indicates heart tissues. *C*: steady state levels of *Ano5* mRNA were measured from heart of 3-mo-old WT male and female male; $n = 4$ animals. Relative expression was normalized to a housekeeping gene, *Hprt*, and resulting values were compared with the level of *Ano5* mRNA levels in hearts of 3-mo-old males. Data are represented as means ± SE. Welch's *t* test was performed to determine statistical significance. $^{**}P < 0.01$. ANO5, Anoctamin-5; WT, wild type.

DATA AVAILABILITY

All data generated or analyzed during this study are included in this published article and its supplementary information files.

SUPPLEMENTAL DATA

Supplemental Files S1–S5: https://doi.org/10.6084/m9.figshare.16661206.v3.

ACKNOWLEDGMENTS

We thank Dr. Jeffrey Boatright and Preston Girardot for sharing treadmills and advising treadmill experiments, Dr. Yuanyuan Cui for assistance with RT-PCR, and Emory Undergraduate students including Grace Lee, Carol Zhu, and Neil Reddy for technical assistance.

GRANTS

This research was supported by grants from the National Institutes of Health: the National Institute of Arthritis and Musculoskeletal Diseases awards R01AR071397 (to H.J.C.) and F32AR074249 (to S.J.F.), National Eye Institute under award number R01EY114852 (to H.C.H.), and the National Institute of General Medical Sciences Grant R01GM132598 (to H.C.H.). Echocardiography for this study was supported in part by the Emory Animal Physiology Core, which is subsidized by Emory University and Children's Healthcare of Atlanta. Additional support was provided by the Office of the Director of the National Institutes of Health under Award Number S10OD021748.

DISCLOSURES

No conflicts of interest, financial or otherwise, are declared by the authors.

AUTHOR CONTRIBUTIONS

H.J.C. conceived and designed research; S.F., F.W., and N.G. performed experiments; S.F., F.W., N.G., J.K., and H.J.C. analyzed data; S.F., F.W., N.G., J.K., and H.J.C. interpreted results of experiments; S.F., J.K., and H.J.C. prepared figures; S.F. and H.J.C. drafted manuscript; S.F., J.K., H.C.H., and H.J.C. edited and revised manuscript; S.F., F.W., N.G., J.K., H.C.H., and H.J.C. approved final version of manuscript.

REFERENCES

1. **Bolduc V**, **Marlow G**, **Boycott KM**, **Saleki K**, **Inoue H**, **Kroon J**, **Itakura M**, **Robitaille Y**, **Parent L**, **Baas F**, **Mizuta K**, **Kamata N**, **Richard I**, **Linssen WH**, **Mahjneh I**, **de Visser M**, **Bashir R**, **Brais B.** Recessive mutations in the putative calcium-activated chloride channel Anoctamin 5 cause proximal LGMD2L and distal MMD3 muscular dystrophies. *Am J Hum Genet* 86: 213–221, 2010. doi:10.1016/j.ajhg.2009.12.013.
2. **Mahjneh I**, **Jaiswal J**, **Lamminen A**, **Somer M**, **Marlow G**, **Kiuru-Enari S**, **Bashir R.** A new distal myopathy with mutation in anoctamin 5. *Neuromuscul Disord* 20: 791–795, 2010. doi:10.1016/j.nmd.2010.07.270.
3. **Hicks D**, **Sarkozy A**, **Muelas N**, **Köehler K**, **Huebner A**, **Hudson G**, **Chinnery PF**, **Barresi R**, **Eagle M**, **Polvikoski T**, **Bailey G**, **Miller J**, **Radunovic A**, **Hughes PJ**, **Roberts R**, **Krause S**, **Walter MC**, **Laval SH**, **Straub V**, **Lochmüller H**, **Bushby K.** A founder mutation in Anoctamin 5 is a major cause of limb-girdle muscular dystrophy. *Brain* 134: 171–182, 2011. doi:10.1093/brain/awq294.
4. **Nallamilli BRR**, **Chakravorty S**, **Kesari A**, **Tanner A**, **Ankala A**, **Schneider T**, **da Silva C**, **Beadling R**, **Alexander JJ**, **Askree SH**, **Whitt Z**, **Bean L**, **Collins C**, **Khadilkar S**, **Gaitonde P**, **Dastur R**, **Wicklund M**, **Mozaffar T**, **Harms M**, **Rufibach L**, **Mittal P**, **Hegde M.** Genetic landscape and novel disease mechanisms from a large LGMD cohort of 4656 patients. *Ann Clin Transl Neurol* 5: 1574–1587, 2018. doi:10.1002/acn3.649.
5. **Papadopoulos C**, **LaforÊt P**, **Nectoux J**, **Stojkovic T**, **Wahbi K**, **Carlier RY**, **Carlier PG**, **Leonard-Louis S**, **Leturcq F**, **Romero N**, **Eymard B**, **Behin A.** Hyperckemia and myalgia are common presentations of anoctamin-5-related myopathy in French patients. *Muscle Nerve* 56: 1096–1100, 2017. doi:10.1002/mus.25608.
6. **Srinivasan R**, **Yun P**, **Neuhaus S**, **Mohassel P**, **Dastgir J**, **Donkervoort S**, **Schindler A**, **Mankodi A**, **Foley AR**, **Arai AE**, **Bönnemann CG.** Cardiac MRI identifies valvular and myocardial disease in a subset of ANO5-related muscular dystrophy patients. *Neuromuscul Disord* 30: 742–749, 2020. doi:10.1016/j.nmd.2020.07.001.
7. **Wahbi K**, **Béhin A**, **Bécane HM**, **Leturcq F**, **Cossée M**, **Laforêt P**, **Stojkovic T**, **Carlier P**, **Toussaint M**, **Gaxotte V**, **Cluzel P**, **Eymard B**, **Duboc D.** Dilated cardiomyopathy in patients with mutations in anoctamin 5. *Int J Cardiol* 168: 76–79, 2013. doi:10.1016/j.ijcard.2012.09.070.
8. **Witting N**, **Duno M**, **Petri H**, **Krag T**, **Bundgaard H**, **Kober L**, **Vissing J.** Anoctamin 5 muscular dystrophy in Denmark: prevalence, genotypes, phenotypes, cardiac findings, and muscle protein expression. *J Neurol* 260: 2084–2093, 2013. doi:10.1007/s00415-013-6934-y.
9. **Bazrafshan S**, **Kushlaf H**, **Kakroo M**, **Quinlan J**, **Becker RC**, **Sadayappan S.** Genetic modifiers of hereditary neuromuscular disorders and cardiomyopathy. *Cells* 10: 349, 2021. doi:10.3390/cells10020349.
10. **Moksnes MR**, **Røsjø H**, **Richmond A**, **Lyngbakken MN**, **Graham SE**, **Hansen AF**, **Wolford BN**, **Gagliano Taliun SA**, **LeFaive J**, **Rasheed H**, **Thomas LF**, **Zhou W**, **Aung N**, **Surakka I**, **Douville NJ**, **Campbell A**, **Porteous DJ**, **Petersen SE**, **Munroe PB**, **Welsh P**, **Sattar N**, **Smith GD**, **Fritsche LG**, **Nielsen JB**, **Åsvold BO**, **Hveem K**, **Hayward C**, **Willer CJ**, **Brumpton BM**, **Omland , T.** Genome-wide association study of cardiac troponin I in the general population. *Hum Mol Genet* 30: 2027–2039, 2021. doi:10.1093/hmg/ddab124.
11. **Caputo A**, **Caci E**, **Ferrera L**, **Pedemonte N**, **Barsanti C**, **Sondo E**, **Pfeffer U**, **Ravazzolo R**, **Zegarra-Moran O**, **Galietta LJ.** TMEM16A, a membrane protein associated with calcium-dependent chloride channel activity. *Science* 322: 590–594, 2008. doi:10.1126/science.1163518.
12. **Schroeder BC**, **Cheng T**, **Jan YN**, **Jan LY.** Expression cloning of TMEM16A as a calcium-activated chloride channel subunit. *Cell* 134: 1019–1029, 2008. doi:10.1016/j.cell.2008.09.003.
13. **Whitlock JM**, **Hartzell HC.** Anoctamins/TMEM16 proteins: chloride channels flirting with lipids and extracellular vesicles. *Annu Rev Physiol* 79: 119–143, 2017. doi:10.1146/annurev-physiol-022516-034031.
14. **Yu K**, **Whitlock JM**, **Lee K**, **Ortlund EA**, **Cui YY**, **Hartzell HC.** Identification of a lipid scrambling domain in ANO6/TMEM16F. *eLife* 4: e06901, 2015. doi:10.7554/eLife.06901.
15. **Whitlock JM**, **Hartzell HC.** A Pore Idea: the ion conduction pathway of TMEM16/ANO proteins is composed partly of lipid. *Pflugers Arch* 468: 455–473, 2016. doi:10.1007/s00424-015-1777-2.
16. **Whitlock JM**, **Yu K**, **Cui YY**, **Hartzell HC.** Anoctamin 5/TMEM16E facilitates muscle precursor cell fusion. *J Gen Physiol* 150: 1498–1509, 2018. doi:10.1085/jgp.201812097.
17. **Griffin DA**, **Johnson RW**, **Whitlock JM**, **Pozsgai ER**, **Heller KN**, **Grose WE**, **Arnold WD**, **Sahenk Z**, **Hartzell HC**, **Rodino-Klapac LR.** Defective membrane fusion and repair in Anoctamin5-deficient muscular dystrophy. *Hum Mol Genet* 25: 1900–1911, 2016. doi:10.1093/hmg/ddw063.
18. **Foltz SJ**, **Cui YY**, **Choo HJ**, **Hartzell HC.** ANO5 ensures trafficking of annexins in wounded myofibers. *J Cell Biol* 220: e202007059, 2021. doi:10.1083/jcb.202007059.
19. **Savarese M**, **Di Fruscio G**, **Tasca G**, **Ruggiero L**, **Janssens S**, **De Bleecker J**, **Delpech M**, **Musumeci O**, **Toscano A**, **Angelini C**, **Sacconi S**, **Santoro L**, **Ricci E**, **Claes K**, **Politano L**, **Nigro V.** Next generation sequencing on patients with LGMD and nonspecific myopathies: findings associated with ANO5 mutations. *Neuromuscul Disord* 25: 533–541, 2015. doi:10.1016/j.nmd.2015.03.011.
20. **Sarkozy A**, **Hicks D**, **Hudson J**, **Laval SH**, **Barresi R**, **Hilton-Jones D**, et al**.** ANO5 gene analysis in a large cohort of patients with anoctaminopathy: confirmation of male prevalence and high occurrence of the common exon 5 gene mutation. *Hum Mutat* 34: 1111–1118, 2013. doi:10.1002/humu.22342.
21. **Livak KJ**, **Schmittgen TD.** Analysis of relative gene expression data using real-time quantitative PCR and the 2(-Delta C(T)) method. *Methods* 25: 402–408, 2001. doi:10.1006/meth.2001.1262.
22. **Schiaffino S**, **Gorza L**, **Sartore S**, **Saggin L**, **Ausoni S**, **Vianello M**, **Gundersen K**, **Lømo T.** Three myosin heavy chain isoforms in type 2 skeletal muscle fibres. *J Muscle Res Cell Motil* 10: 197–205, 1989. doi:10.1007/BF01739810.
23. **Putman CT**, **Xu X**, **Gillies E**, **MacLean IM**, **Bell GJ.** Effects of strength, endurance and combined training on myosin heavy chain content and fibre-type distribution in humans. *Eur J Appl Physiol* 92: 376–384, 2004. doi:10.1007/s00421-004-1104-7.
24. **Encarnacion-Rivera L**, **Foltz S**, **Hartzell HC**, **Choo H.** Myosoft: an automated muscle histology analysis tool using machine learning algorithm utilizing FIJI/ImageJ software. *PLoS One* 15: e0229041, 2020. doi:10.1371/journal.pone.0229041.
25. **Vilquin JT**, **Brussee V**, **Asselin I**, **Kinoshita I**, **Gingras M**, **Tremblay JP.** Evidence of mdx mouse skeletal muscle fragility in vivo by eccentric running exercise. *Muscle Nerve* 21: 567–576, 1998. doi:10.1002/(SICI)1097-4598(199805)21:5<567::AID-MUS2>3.0.CO;2-6.
26. **Ghazal N**, **Peoples JN**, **Mohiuddin TA**, **Kwong JQ.** Mitochondrial functional resilience after TFAM ablation in the adult heart. *Am J Physiol Cell Physiol* 320: C929–C942, 2021. doi:10.1152/ajpcell.00508.2020.
27. **Khawajazada T**, **Kass K**, **Rudolf K**, **de Stricker Borch J**, **Sheikh AM**, **Witting N**, **Vissing J.** Muscle involvement assessed by quantitative magnetic resonance imaging in patients with anoctamin 5 deficiency. *Eur J Neurol* 28: 3121–3132, 2021. doi:10.1111/ene.14979.
28. **Vázquez J**, **Lefeuvre C**, **Escobar RE**, **Luna Angulo AB**, **Miranda Duarte A**, **Delia Hernandez A**, **Brisset M**, **Carlier RY**, **Leturcq F**, **Durand-Canard MC**, **Nicolas G**, **Laforet P**, **Malfatti E.** Phenotypic spectrum of myopathies with recessive Anoctamin-5 mutations. *J Neuromuscul Dis* 7: 443–451, 2020. doi:10.3233/JND-200515.
29. **Seguí F**, **Gonzalez-Quereda L**, **Sanchez A**, **Matas-García A**, **Garrabou G**, **Rodriguez MJ**, **Gallano P**, **Grau JM**, **Milisenda JC.** Anoctamin 5 (ANO5) muscular dystrophy-three different phenotypes and a new histological pattern. *Neurol Sci* 41: 2967–2971, 2020. doi:10.1007/s10072-020-04453-y.
30. **Panadés-de Oliveira L**, **Bermejo-Guerrero L**, **de Fuenmayor-Fernández de la Hoz CP**, **Cantero Montenegro D**, **Hernández Lain A**, **Martí P**, **Muelas N**, **Vílchez JJ**, **Domínguez-González C.** Persistent asymptomatic or mild symptomatic hyperCKemia due to mutations in ANO5: the mildest end of the anoctaminopathies spectrum. *J Neurol* 267: 2546–2555, 2020. doi:10.1007/s00415-020-09872-7.
31. **Jarmula A**, **Łusakowska A**, **Fichna JP**, **Topolewska M**, **Macias A**, **Johnson K**, **Töpf A**, **Straub V**, **Rosiak E**, **Szczepaniak K**, **Dunin-Horkawicz S**, **Maruszak A**, **Kaminska AM**, **Redowicz MJ.** ANO5 mutations in the Polish limb girdle muscular dystrophy patients:

effects on the protein structure. *Sci Rep* 9: 11533, 2019. doi:10.1038/s41598-019-47849-3.

32. **Silva AMS**, **Coimbra-Neto AR**, **Souza PVS**, **Winckler PB**, **Gonçalves MVM**, **Cavalcanti EBU**, **Carvalho AADS**, **Sobreira CFDR**, **Camelo CG**, **Mendonça RDH**, **Estephan EDP**, **Reed UC**, **Machado-Costa MC**, **Dourado-Junior MET**, **Pereira VC**, **Cruzeiro MM**, **Helito PVP**, **Aivazoglou LU**, **Camargo LVD**, **Gomes HH**, **Camargo AJSD**, **Pinto WBVDR**, **Badia BML**, **Libardi LH**, **Yanagiura MT**, **Oliveira ASB**, **Nucci A**, **Saute JAM**, **França-Junior MC**, **Zanoteli E.** Clinical and molecular findings in a cohort of ANO5-related myopathy. *Ann Clin Transl Neurol* 6: 1225–1238, 2019. doi:10.1002/acn3.50801.
33. **Cai S**, **Gao M**, **Xi J**, **Liu Z**, **Yue D**, **Wu H**, **Bi H**, **Li J**, **Liang Z**, **Zhao C**, **Udd B**, **Luo S**, **Lu J.** Clinical spectrum and gene mutations in a Chinese cohort with anoctaminopathy. *Neuromuscul Disord* 29: 628–633, 2019. doi:10.1016/j.nmd.2019.06.005.
34. **Ten Dam L**, **Frankhuizen WS**, **Linssen W**, **Straathof CS**, **Niks EH**, **Faber K**, **Fock A**, **Kuks JB**, **Brusse E**, **de Coo R**, **Voermans N**, **Verrips A**, **Hoogendijk JE**, **van der Pol L**, **Westra D**, **de Visser M**, **van der Kooi AJ**, **Ginjaar I.** Autosomal recessive limb-girdle and Miyoshi muscular dystrophies in the Netherlands: the clinical and molecular spectrum of 244 patients. *Clin Genet* 96: 126–133, 2019. doi:10.1111/cge.13544.
35. **Ylikallio E**, **Auranen M**, **Mahjneh I**, **Lamminen A**, **Kousi M**, **Träskelin AL**, **Muurinen T**, **Löfberg M**, **Salmi T**, **Paetau A**, **Lehesjoki AE**, **Piirilä P**, **Kiuru-Enari S.** Decreased aerobic capacity in ANO5-muscular dystrophy. *J Neuromuscul Dis* 3: 475–485, 2016. doi:10.3233/JND-160186.
36. **Liewluck T**, **Winder TL**, **Dimberg EL**, **Crum BA**, **Heppelmann CJ**, **Wang Y**, **Bergen HR 3rd**, **Milone M.** ANO5-muscular dystrophy: clinical, pathological and molecular findings. *Eur J Neurol* 20: 1383–1389, 2013. doi:10.1111/ene.12191.
37. **van der Kooi AJ**, **Ten Dam L**, **Frankhuizen WS**, **Straathof CS**, **van Doorn PA**, **de Visser M**, **Ginjaar IB.** ANO5 mutations in the Dutch limb girdle muscular dystrophy population. *Neuromuscul Disord* 23: 456–460, 2013. doi:10.1016/j.nmd.2013.03.012.
38. **Schessl J**, **Kress W**, **Schoser B.** Novel ANO5 mutations causing hyper-CK-emia, limb girdle muscular weakness and Miyoshi type of muscular dystrophy. *Muscle Nerve* 45: 740–742, 2012. doi:10.1002/mus.23281.
39. **Sarkozy A**, **Deschauer M**, **Carlier RY**, **Schrank B**, **Seeger J**, **Walter MC**, **Schoser B**, **Reilich P**, **Leturq F**, **Radunovic A**, **Behin A**, **Laforet P**, **Eymard B**, **Schreiber H**, **Hicks D**, **Vaidya SS**, **Gläser D**, **Carlier PG**, **Bushby K**, **Lochmüller H**, **Straub V.** Muscle MRI findings in limb girdle muscular dystrophy type 2L. *Neuromuscul Disord* 22*Suppl 2*: S122–S129, 2012. doi:10.1016/j.nmd.2012.05.012.
40. **Magri F**, **Del Bo R**, **D'Angelo MG**, **Sciacco M**, **Gandossini S**, **Govoni A**, **Napoli L**, **Ciscato P**, **Fortunato F**, **Brighina E**, **Bonato S**, **Bordoni A**, **Lucchini V**, **Corti S**, **Moggio M**, **Bresolin N**, **Comi GP.** Frequency and characterisation of anoctamin 5 mutations in a cohort of Italian limb-girdle muscular dystrophy patients. *Neuromuscul Disord* 22: 934–943, 2012. doi:10.1016/j.nmd.2012.05.001.
41. **Bansal D**, **Miyake K**, **Vogel SS**, **Groh S**, **Chen CC**, **Williamson R**, **McNeil PL**, **Campbell KP.** Defective membrane repair in dysferlin-deficient muscular dystrophy. *Nature* 423: 168–172, 2003. doi:10.1038/nature01573.
42. **Swaggart KA**, **Demonbreun AR**, **Vo AH**, **Swanson KE**, **Kim EY**, **Fahrenbach JP**, **Holley-Cuthrell J**, **Eskin A**, **Chen Z**, **Squire K**, **Heydemann A**, **Palmer AA**, **Nelson SF**, **McNally EM.** Annexin A6 modifies muscular dystrophy by mediating sarcolemmal repair. *Proc Natl Acad Sci USA* 111: 6004–6009, 2014. doi:10.1073/pnas.1324242111.
43. **Demonbreun AR**, **Quattrocelli M**, **Barefield DY**, **Allen MV**, **Swanson KE**, **McNally EM.** An actin-dependent annexin complex mediates plasma membrane repair in muscle. *J Cell Biol* 213: 705–718, 2016. doi:10.1083/jcb.201512022.
44. **Demonbreun AR**, **Fallon KS**, **Oosterbaan CC**, **Bogdanovic E**, **Warner JL**, **Sell JJ**, **Page PG**, **Quattrocelli M**, **Barefield DY**, **McNally EM.** Recombinant annexin A6 promotes membrane repair and protects against muscle injury. *J Clin Invest* 129: 4657–4670, 2019. doi:10.1172/JCI128840.
45. **Griffin DA**, **Johnson RW**, **Whitlock JM**, **Pozsgai ER**, **Heller KN**, **Grose WE**, **Arnold WD**, **Sahenk Z**, **Hartzell HC**, **Rodino-Klapac LR.** Defective membrane fusion and repair in Anoctamin5-deficient muscular dystrophy. *Hum Mol Genet* 25: 1900–1911, 2016. doi:10.1093/hmg/ddw063.
46. **Middel V**, **Zhou L**, **Takamiya M**, **Beil T**, **Shahid M**, **Roostalu U**, **Grabher C**, **Rastegar S**, **Reischl M**, **Nienhaus GU**, **Strähle U.** Dysferlin-mediated phosphatidylserine sorting engages macrophages in sarcolemma repair. *Nat Commun* 7: 12875, 2016. doi:10.1038/ncomms12875.
47. **Carmeille R**, **Bouvet F**, **Tan S**, **Croissant C**, **Gounou C**, **Mamchaoui K**, **Mouly V**, **Brisson AR**, **Bouter A.** Membrane repair of human skeletal muscle cells requires Annexin-A5. *Biochim Biophys Acta* 1863: 2267–2279, 2016. doi:10.1016/j.bbamcr.2016.06.003.
48. **Buckingham M.** Gene regulatory networks and cell lineages that underlie the formation of skeletal muscle. *Proc Natl Acad Sci USA* 114: 5830–5837, 2017. doi:10.1073/pnas.1610605114.
49. **Tsutsumi S**, **Kamata N**, **Vokes TJ**, **Maruoka Y**, **Nakakuki K**, **Enomoto S**, **Omura K**, **Amagasa T**, **Nagayama M**, **Saito-Ohara F**, **Inazawa J**, **Moritani M**, **Yamaoka T**, **Inoue H**, **Itakura M.** The novel gene encoding a putative transmembrane protein is mutated in gnathodiaphyseal dysplasia (GDD). *Am J Hum Genet* 74: 1255–1261, 2004. doi:10.1086/421527.
50. **Penttila S**, **Vihola A**, **Palmio J**, **Udd B.** ANO5 muscle disease. In: *GeneReviews((R))*, edited by Adam MP, Ardinger HH, Pagon RA, Wallace SE, Bean LJH, Mirzaa G, Amemiya A. Seattle, WA: University of Washington, 1993–2022**.**
51. **Monjaret F**, **Suel-Petat L**, **Bourg-Alibert N**, **Vihola A**, **Marchand S**, **Roudaut C**, **Gicquel E**, **Udd B**, **Richard I**, **Charton K.** The phenotype of dysferlin-deficient mice is not rescued by adeno-associated virus-mediated transfer of anoctamin 5. *Hum Gene Ther Clin Dev* 24: 65–76, 2013. doi:10.1089/humc.2012.217.
52. **Harris E**, **Bladen CL**, **Mayhew A**, **James M**, **Bettinson K**, **Moore U**, et al**.** The Clinical Outcome Study for dysferlinopathy: an international multicenter study. *Neurol Genet* 2: e89, 2016. doi:10.1212/NXG.0000000000000089.
53. **Han R**, **Bansal D**, **Miyake K**, **Muniz VP**, **Weiss RM**, **McNeil PL**, **Campbell KP.** Dysferlin-mediated membrane repair protects the heart from stress-induced left ventricular injury. *J Clin Invest* 117: 1805–1813, 2007. doi:10.1172/JCI30848.
54. **Chase TH**, **Cox GA**, **Burzenski L**, **Foreman O**, **Shultz LD.** Dysferlin deficiency and the development of cardiomyopathy in a mouse model of limb-girdle muscular dystrophy 2B. *Am J Pathol* 175: 2299–2308, 2009. doi:10.2353/ajpath.2009.080930.
55. **Grounds MD**, **Terrill JR**, **Radley-Crabb HG**, **Robertson T**, **Papadimitriou J**, **Spuler S**, **Shavlakadze T.** Lipid accumulation in dysferlin-deficient muscles. *Am J Pathol* 184: 1668–1676, 2014. doi:10.1016/j.ajpath.2014.02.005.
56. **Kuru S**, **Yasuma F**, **Wakayama T**, **Kimura S**, **Konagaya M**, **Aoki M**, **Tanabe M**, **Takahashi T.** [A patient with limb girdle muscular dystrophy type 2B (LGMD2B) manifesting cardiomyopathy]. *Rinsho Shinkeigaku* 44: 375–378, 2004.
57. **Wenzel K**, **Geier C**, **Qadri F**, **Hubner N**, **Schulz H**, **Erdmann B**, **Gross V**, **Bauer D**, **Dechend R**, **Dietz R**, **Osterziel KJ**, **Spuler S**, **Ozcelik C.** Dysfunction of dysferlin-deficient hearts. *J Mol Med (Berl)* 85: 1203–1214, 2007. doi:10.1007/s00109-007-0253-7.
58. **Hegde S**, **Maysky M**, **Zaidi A.** A rare case of lead-induced cardiomyopathy. *JACC Case Rep* 2: 1496–1500, 2020. doi:10.1016/j.jaccas.2020.05.047.
59. **Adamo CM**, **Dai DF**, **Percival JM**, **Minami E**, **Willis MS**, **Patrucco E**, **Froehner SC**, **Beavo JA.** Sildenafil reverses cardiac dysfunction in the mdx mouse model of Duchenne muscular dystrophy. *Proc Natl Acad Sci USA* 107: 19079–19083, 2010. doi:10.1073/pnas.1013077107.
60. **Fayssoil A**, **Renault G**, **Guerchet N**, **Marchiol-Fournigault C**, **Fougerousse F**, **Richard I.** Cardiac characterization of mdx mice using high-resolution doppler echocardiography. *J Ultrasound Med* 32: 757–761, 2013. doi:10.7863/ultra.32.5.757.
61. **Mavrogeni S**, **Markousis-Mavrogenis G**, **Papavasiliou A**, **Kolovou G.** Cardiac involvement in Duchenne and Becker muscular dystrophy. *World J Cardiol* 7: 410–414, 2015. doi:10.4330/wjc.v7.i7.410.
62. **Durbeej M**, **Cohn RD**, **Hrstka RF**, **Moore SA**, **Allamand V**, **Davidson BL**, **Williamson RA**, **Campbell KP.** Disruption of the beta-sarcoglycan gene reveals pathogenetic complexity of limb-girdle muscular dystrophy type 2E. *Mol Cell* 5: 141–151, 2000. doi:10.1016/s1097-2765(00)80410-4.

63. **Andersson DC**, **Meli AC**, **Reiken S**, **Betzenhauser MJ**, **Umanskaya A**, **Shiomi T**, **D'Armiento J**, **Marks AR.** Leaky ryanodine receptors in beta-sarcoglycan deficient mice: a potential common defect in muscular dystrophy. *Skelet Muscle* 2: 9, 2012. doi:10.1186/2044-5040-2-9.
64. **Barresi R**, **Di Blasi C**, **Negri T**, **Brugnoni R**, **Vitali A**, **Felisari G**, **Salandi A**, **Daniel S**, **Cornelio F**, **Morandi L**, **Mora M.** Disruption of heart sarcoglycan complex and severe cardiomyopathy caused by beta sarcoglycan mutations. *J Med Genet* 37: 102–107, 2000. doi:10.1136/jmg.37.2.102.
65. **Sui T**, **Xu L**, **Lau YS**, **Liu D**, **Liu T**, **Gao Y**, **Lai L**, **Han R**, **Li Z.** Development of muscular dystrophy in a CRISPR-engineered mutant rabbit model with frame-disrupting ANO5 mutations. *Cell Death Dis* 9: 609, 2018 [Erratum in *Cell Death Dis* 11: 468, 2020]. doi:10.1038/s41419-018-0674-y.
66. **Ahluwalia J**, **Ly JQ**, **Norman E**, **Costello RF Jr**, **Beall DP.** Gnathodiaphyseal dysplasia. *Clin Imaging* 31: 67–69, 2007. doi:10.1016/j.clinimag.2006.07.003.
67. **Marconi C**, **Brunamonti Binello P**, **Badiali G**, **Caci E**, **Cusano R**, **Garibaldi J**, **Pippucci T**, **Merlini A**, **Marchetti C**, **Rhoden KJ**, **Galietta LJ**, **Lalatta F**, **Balbi P**, **Seri M.** A novel missense mutation in ANO5/TMEM16E is causative for gnathodiaphyseal dyplasia in a large Italian pedigree. *Eur J Hum Genet* 21: 613–619, 2013. doi:10.1038/ejhg.2012.224.
68. **Di Zanni E**, **Gradogna A**, **Scholz-Starke J**, **Boccaccio A.** Gain of function of TMEM16E/ANO5 scrambling activity caused by a mutation associated with gnathodiaphyseal dysplasia. *Cell Mol Life Sci* 75: 1657–1670, 2018. doi:10.1007/s00018-017-2704-9.
69. **Di Zanni E**, **Gradogna A**, **Picco C**, **Scholz-Starke J**, **Boccaccio A.** TMEM16E/ANO5 mutations related to bone dysplasia or muscular dystrophy cause opposite effects on lipid scrambling. *Hum Mutat* 41: 1157–1170, 2020. doi:10.1002/humu.24006.
70. **Rahit K**, **Tarailo-Graovac M.** Genetic modifiers and rare Mendelian disease. *Genes (Basel)* 11: 239, 2020. doi:10.3390/genes11030239.